AIAA JOURNAL
Vol. 35, No. 3, March 1997

Algebraic Turbulence Modeling for Swept Shock-Wave/Turbulent Boundary-Layer Interactions

Argyris G. Panaras*
DLR, German Aerospace Research Establishment, D-37073 Göttingen, Germany

New algebraic turbulence modeling is derived that is appropriate for the simulation of swept shock-wave/turbulent boundary-layer interactions. In the quasiconical separation vortex, which appears in these types of flows, the low-intermittency outer part of the boundary layer rotates around the core of the vortex and penetrates into the separation bubble at the reattachment region, forming a low-turbulence tongue that lies along the surface under the vortex. This physical feature was considered in the derivation of a new equation for calculation of the eddy-viscosity coefficient in the region of the separation vortex. The Baldwin–Lomax formulation is followed, because it is easily implemented in a Navier–Stokes computation scheme. Also, an alternative eddy-viscosity coefficient is presented that is closer to Clauser's linear relation than the original Baldwin–Lomax relations. The proposed calculation scheme is completed by a simple rule for calculation of the thickness of the boundary layer in types of flows where, because of the existence of shock waves and mixing layers, multiple maxima exist in the moment of vorticity profiles. Application of the new turbulence modeling in supersonic sharp-fin–plate flows resulted in good agreement with the experimental evidence. Also, a preliminary application of the new relations to a crossing shock configuration indicated that this complex flow can be simulated quite well.

I. Introduction

THE interaction of a swept shock wave with a turbulent boundary layer is studied, experimentally and computationally, in many simple configurations that resemble critical regions of a high-speed vehicle. The simplest configuration consists of a sharp fin attached normally to a flat plate at a certain distance behind its leading edge. The swept shock wave generated by the fin interacts with the boundary layer on the plate and, if it is sufficiently strong, a quasiconical flattened separation vortex is formed, overlaid by a λ-shock.[1] The conical vortex carries high-energy air from the external flow to its reattachment region, causing the appearance of peak heating and high values of pressure in this region. The structure of the flow about a fin–plate configuration is described in detail in the reviews of Knight,[2] Settler,[3] and Panaras.[4]

Although the numerical simulations of flows about sharp-fin–plate configurations have contributed considerably to understanding the nature of these flows, the accuracy of the predictions still is not very high. In various Navier–Stokes calculations, which employ the algebraic turbulence models of Cebeci and Smith[5] and of Baldwin and Lomax[6] and the two-equation κ–ε model, it has been found that the computations agree well with the data for moderate interaction strengths but systematically underpredict the size of the interaction domain and fail to predict the secondary separation with increasing interaction strength (see review of Knight[2] and the paper of Kim et al.[7]). Panaras and Stanewsky[8] have shown that accurate results are provided only by a version of the Baldwin–Lomax model, originally proposed by Degani and Schiff[9] for high-angle-of-attack aerodynamics, according to which the separation vortex is excluded from calculation of the eddy-viscosity coefficients (cutoff turbulence model).

In a recent work, Panaras[10] has studied the effect on turbulence modeling of the structure of the separation vortex, which appears in a strong swept shock-wave/turbulent boundary-layer interaction. For this, the cutoff turbulence model war applied to a well-documented sharp-fin–plate flow.[11] After validation of the results, by comparison with appropriate experimental data, he studied the flowfield by means of stream surfaces, which start at the inflow plane, within the undisturbed boundary layer, and that are initially parallel to the plate. Each of these surfaces has been represented by a number of streamlines. Calculation of the spatial evolution of some selected stream surfaces has revealed that the inner layers of the undisturbed boundary layer, where the eddy viscosity is high, wind around the core of the vortex. However, the outer layers, which have low turbulence, rotate over the vortex and penetrate into the separation bubble at the reattachment region, forming a low-turbulence tongue that lies along the plate under the vortex. The intermittency of the air that constitutes the tongue is very small, i.e., the flow is almost laminar there. At the initial stage of development, the conical vortex is composed completely of turbulent air, but gradually downstream, as it grows linearly, the low-turbulence tongue is formed. When additional test cases were studied, it was found that increasing the strength of the interaction results in folding around the vortex of higher, purely inviscid layers. At the other extreme, in a weak interaction, no low-turbulence tongue is formed (see Fig. 1, taken from Ref. 10). Panaras[10] has shown that the remarkable success of calculations in which the vortex is excluded from estimation of the eddy-viscosity coefficients is due to the fact that, in the region of the low-turbulence tongue, the cutoff model predicts very small values of the eddy-viscosity coefficient.

The existence of the low-turbulence tongue under the conical separation vortex of a strong swept-shock/turbulent boundary layer interaction creates a mixed-type separation bubble: turbulent in the region of the separation line and almost laminar between the reattachment line and the secondary separation vortex. This type of separation cannot possibly be simulated accurately with the presently used algebraic turbulence models, because the basic relations of these models are based on the physics of two-dimensional flows where, in a separation bubble, the whole recirculation region is turbulent. For improving the accuracy of the numerical predictions of swept shock-wave/turbulent boundary-layer interactions, a new equation for calculation of the eddy viscosity in the separation region is developed in this paper, which considers the mixed character of the conical vortex. The sharp-fin–plate is considered as the prototype flow configuration. Also, the basic formulation introduced by Baldwin and Lomax[6] is followed because it is more easily implemented in a Navier–Stokes computation scheme than other algebraic turbulence models. The developed model is used for computation of some of the test cases compiled by Settles and Dodson.[11] The agreement with the experimental data is very good. Also some preliminary results for a crossing-shock interaction are presented.

Received April 17, 1996; revision received Sept. 5, 1996; accepted for publication Dec. 4, 1996; also published in *AIAA Journal on Disc*, Volume 2, Number 2.

*Visiting Scientist, Institute for Fluid Mechanics, Bunsenstrasse 10; currently Consulting Engineer, Agias, Elenis 63, Athens 15772, Greece. Associate Fellow AIAA.

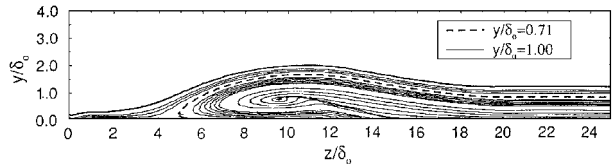

a) $M_0 = 3.0$ and $\alpha = 10$ deg

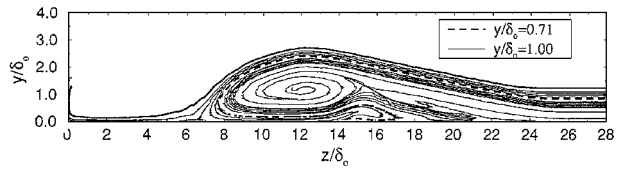

b) $M_0 = 3.0$ and $\alpha = 16$ deg

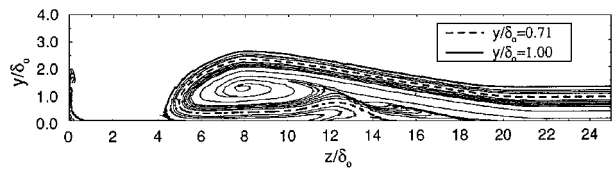

c) $M_0 = 4.0$ and $\alpha = 16$ deg

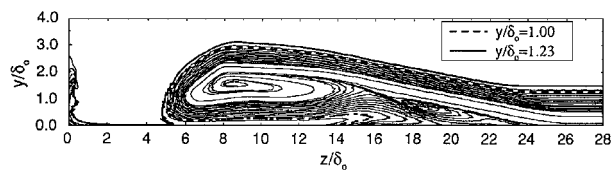

d) $M_0 = 4.0$ and $\alpha = 20$ deg

Fig. 1 Cross-sections of various fin–plate flows.[10]

II. Baldwin–Lomax Algebraic Turbulence Model

In the inner layer, Baldwin and Lomax[6] use the Prandlt–van Driest formulation

$$(\mu_t)_{\text{inner}} = \rho(\kappa D\eta)^2\omega \tag{1}$$

where κ is the von Kármán constant (equal to 0.41), D is the van Driest damping factor, ω is the absolute value of the vorticity, and η is the distance normal to the wall.

In the outer region, the following equation is used:

$$(\mu_t)_{\text{outer}} = C_{\text{cp}}(0.0168\rho F_{\text{wake}}\gamma)$$
$$F_{\text{wake}} = \text{the smaller of} \begin{cases} \eta_{\max} F_{\max} \\ \dfrac{C_{\text{wk}}\eta_{\max} u_{\text{dif}}^2}{F_{\max}} \end{cases} \tag{2}$$

The quantity $F_{\max}$ is the maximum value of the function $F(\eta) = \eta\omega D$, and $\eta_{\max}$ is the value of η at which it occurs. The Klebanoff intermittency factor γ is given by

$$\gamma = [1 + 5.5(\eta/\delta)^6]^{-1} \tag{3}$$

The quantity u_{dif} is the difference between maximum and minimum velocity in the profile. The thickness of the boundary layer is defined by $\delta = \eta_{\max}/C_{\text{kleb}}$. The constants appearing in the previous relations are $C_{\text{cp}} = 1.6$, $C_{\text{wk}} = 0.25$, and $C_{\text{kleb}} = 0.3$.

For the fin–plate configuration, where there are two intersecting surfaces, a "modified distance" was proposed by Hung and MacCormack[12] to account for the turbulent mixing length near the intersection of the surfaces:

$$\eta = \frac{2yz}{y + z + \sqrt{(y^2 + z^2)}} \tag{4}$$

The calculation procedure introduced by Baldwin and Lomax[6] is very simple. At each surface grid position an outward search is performed along the corresponding normal grid line for the maximum value of the moment of vorticity $F_{\max}$ and the distance from the surface $\eta_{\max}$ where it occurs. Then the thickness of the boundary layer at this particular station is simply equal to $\delta = \eta_{\max}/C_{\text{kleb}}$. The calculation of μ_t from Eqs. (1) and (2) along the examined normal grid line is the final step. However, the simplicity of the calculation procedure is offset, to some extent, by the accuracy of the prediction. Moderate agreement of the model with the experimental evidence has been reported, which has been attributed to various causes, such as the different form of the equation that gives the outer-layer eddy viscosity [Eq. (2)] from the linear formula of Clauser and the erroneous estimation of the thickness of the boundary, layer. In the following section, the particular case of a swept shock-wave/turbulent boundary layer interaction is examined and new relations for the calculation of δ and $(\mu_t)_{\text{outer}}$ are developed.

III. Improved Algebraic Turbulence Modeling

Definition of the Boundary-Layer Thickness

A generalized use of the relation $\delta = \eta_{\max}/C_{\text{kleb}}$ is subjected to the assumption that in any type of flow the maximum of the moment of vorticity appears approximately at $\eta_{\max} = 0.3\delta$. Deriving this value, Baldwin and Lomax[6] reviewed a variety of test cases. This value is not universal. For example, Stock and Haase[13] have shown analytically that in the family of the incompressible Coles profiles the relation $\delta = \eta_{\max}/0.516$ is valid ($\eta_{\max} = 0.516$). The nonexistence of a global correlation between $\eta_{\max}$ and δ led some researchers to develop alternative techniques, which are based on the observation that in incompressible flows the moment of vorticity, F, is zero outside the viscous layer. This topic is reviewed in detail in Johnson,[14] who has tested in transonic flows relations of the type $F/F_{\max} = 0.02\_0.05$ that were originally developed for application in simple incompressible flows, in which rotational regions do not exist outside the boundary layer. He has concluded that these relations are not reliable in transonic flows because residuals exist in the freestream that are due to coarse grids and the presence of shock waves. Examining incompressible and transonic test cases, Johnson[14] found that a reliable criterion is the boundary-layer thickness, δ, defined at $1.2\eta_{1/2}$, where $\eta_{1/2}$ is defined as the location where $F/F_{\max} = 0.5$, and $\eta_{1/2} > \eta_{\max}$.

A model of the structure of a typical fin–plate flow ($M_0 = 4.0$ and $\alpha = 16$ deg) is shown in Fig. 2a, according to Alvi and Settles.[15] They combined planar laser scattering results with wall pressure and skin-friction measurements to construct this model, which visualizes very clearly the λ-shock structure and the shape of the cross section of the separation vortex. The flow modeled in Fig. 2a has been calculated in this work. The calculated moment of vorticity profiles in a crossflow plane are shown in Fig. 2b. It is remarkable that the moment of vorticity profiles also provide good visualization of the shape and size of the cross section of the separation vortex as well as of the shock formation, including the curved shear layer that is formed at the shock triple point and moves toward the corner. The appearance, however, of the signature of the λ-shock structure in the moment of vorticity profiles results in the existence of multiple local maxima, above or below the absolute maximum, $F_{\max}$. The $\eta_{1/2}$ criterion of Johnson does not predict correctly the edge of the boundary layer in some parts of the interaction. In the regions of the shear layer and of the triple-shock point, more than one point exist above $\eta_{\max}$ that have the property of $\eta_{1/2}$.

An optical review of the development of the moment of vorticity profiles shown in Fig. 2b indicates that, along the undisturbed boundary layer and the separation vortex, the line that connects the points that define the edge of the boundary layer is approximately parallel to the line that connects the $\eta_{\max}$ points. This may be interpreted as meaning that in any crossflow profile the distance between the $\eta_{\max}$ point and the edge of the boundary layer is approximately constant. Since in the region of the undisturbed boundary layer the profiles have only one maximum, it is easy to define at a reference crossflow position of this region the $F_{\max}$ and $\eta_{\max}$, which for convenience we note by F_{ref} and η_{ref}, and then to calculate this constant distance from the relation $d_{\text{ref}} = \delta_{\text{ref}} \_ \eta_{\text{ref}} = (1/C_{\text{kleb}} \_ 1)\eta_{\text{ref}}$. Knowledge of d_{ref} gives the possibility of calculating the thickness of the boundary layer in any position of the separation region, where, because of the existence of the λ-shock structure, the previously reviewed methods fail. At any position of the separation region, the thickness of the boundary layer is equal to the sum of $\eta_{\max}$ and of this constant distance d_{ref}.

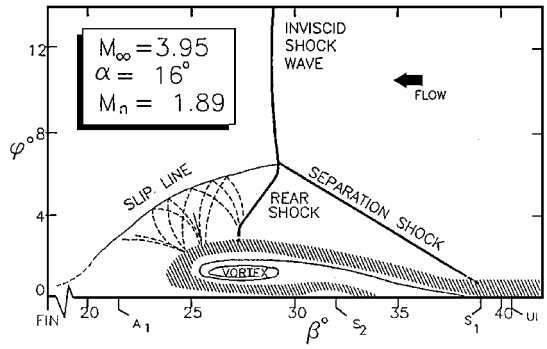

a) Model of Alvi and Settles[15]

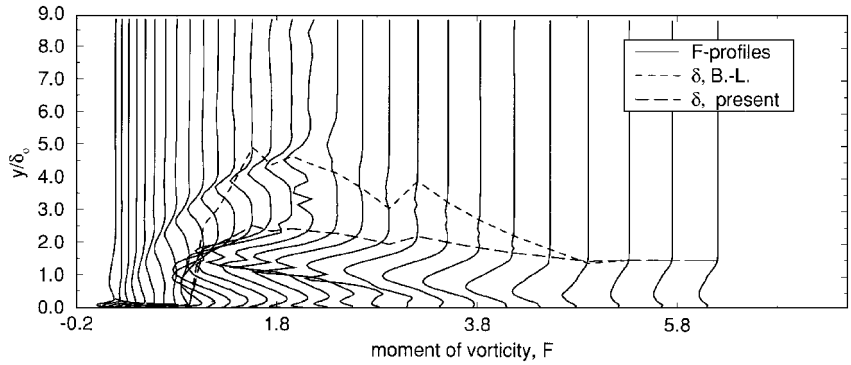

b) Profiles of the moment of vorticity (present calculations)

Fig. 2 Cross-section of a fin–plate flow: $I = 60$.

In summary, the following scheme has been tested for calculation of the edge of the boundary layer in fin–plane flows:

$$\delta = \eta_{\max} + \left(\frac{1}{C_{\text{kleb}}} - 1\right)\eta_{\text{ref}} \quad \text{if} \quad \eta_{\max} > \eta_{\text{ref}}$$
$$\delta = \frac{\eta_{\max}}{C_{\text{kleb}}} \quad \text{if} \quad \eta_{\max} < \eta_{\text{ref}} \tag{5}$$

In Fig. 2b, the present scheme is compared with the standard prediction of the Baldwin–Lomax model, i.e., application of the relation $\delta = \eta_{\max}/C_{\text{kleb}}$ along the extent of the crossflow. It is shown that the present scheme provides a realistic estimation of the edge of the viscous layer; according to the Baldwin–Lomax model the viscous layer extends above the λ-shock formation. With regard to the constant C_{kleb}, the value given by Baldwin and Lomax ($C_{\text{kleb}} = 0.3$) is approximately valid in the undisturbed boundary layer of the supersonic fin–plate flows examined here. This means that the maximum of the moment of vorticity of the attached boundary layer occurs approximately at $\eta = 0.3$, i.e., the value found by Baldwin and Lomax[6] in the data they reviewed. However, I suggest that in a particular application the correctness of this value must be checked during the computation.

The derivation of Eq. (5) is based on the assumption that the boundary layer edge after the flow separates and rotates into a vortex is defined by the trend of the attached boundary layer. This means that the whole cross section of the separation bubble is considered as belonging to the boundary layer. This is a reasonable assumption because, in the model of Baldwin and Lomax,[6] the thickness of the boundary model is used only in the intermittency factor [Eq. (3)] for estimating the degree of turbulence of the flow. Turbulent air exists in the whole extent of a cross section of a separation bubble. Thus, it is correct for the purpose of estimation of the intermittency factor to consider Eq. (5).

According to the data of Fig. 2b, the standard Baldwin–Lomax model overestimates the extent of the viscous turbulent region, covering a region above the separation vortex that actually is purely inviscid. Any solution based on this estimation will be more turbulent compared to the realistic estimation of Eq. (5). However, the primary reason for predicting the high eddy-viscosity values by the Baldwin–Lomax model is the functional form of the relations that give the eddy viscosity in the outer region (wake layer). This statement has been proved by Johnson,[14] who, examining two-dimensional transonic flows, found that the poor agreement of the Baldwin–Lomax model with the experimental evidence is because Eq. (2) does not have the functional form of Clauser's relation

$$(\mu_t)_{\text{outer}} = \alpha\rho U_e \delta^* \tag{6}$$

where U_e is the velocity at the edge of the layer, δ^* is the displacement thickness, and α is a constant.

My initial intention was to develop an appropriate relation for the eddy-viscosity coefficient that follows the physics of the quasiconical separation vortex, which is formed in a strong swept shock-wave/boundary-layer interaction. However, in the course of this study I derived an additional relation for the eddy viscosity, which is closer morphologically to Clauser's equation and can be used for any type of separated flow. The derivation of the two new relations for the eddy-viscosity coefficient is based on the model of flow shown in Fig. 2.

Model 1: Linear Dependence of Eddy Viscosity on Maximum Vorticity

According to the model of Baldwin and Lomax,[6] the eddy viscosity at the outer part of a boundary layer is proportional to the wake function F_{wake}. This function is equal to the minimum of $F_{w1} = \eta_{\max} F_{\max}$ and $F_{w2} = \eta_{\max}/F_{\max}$. If the substitution $F_{\max} = \eta_{\max}\omega_m$ is done, these expressions are written as $F_{m1} = \eta^2_{\max}\omega_m$ and $F_{w2} = 1/\omega_m$. The first expression, F_{m1}, applies to the attached part of a flow, and the second, F_{m2}, to the separated one. In these expressions, ω_m is not equal to the maximum value of ω, but it is a little smaller, because the maximum of the product $\eta\omega$ does not coincide with the maximum of ω. This simple consideration indicates that, in the attached flow, the function F_{wake} depends on the square of $\eta_{\max}$ and it is proportional to ω_m, whereas in the separated flow it has an inverse dependence on ω_m. However, Clauser has proposed for the outer layer a relation that has a linear variation on the displacement thickness of the boundary layer. A similar relation cannot be derived in the Baldwin–Lomax formulation. The only possibility is to derive an expression for the function F_{wake} that is proportional to the vorticity parameter ω_m. Because such a relation has a linear dependence on a boundary-layer parameter, it may be considered close to Clauser's linear-dependence hypothesis.

For deriving an expression for the function F_{wake} that is proportional to ω_n, assume that a reference point is defined upstream of the separation region of the model flow. Then the expression $F_{\text{wake}} = c\eta_{\text{ref}}^2 F_{\max}/\eta_{\max}$ downstream of the reference point has a linear dependence on ω_n and it is scaled by the square of the reference length η_{ref}. This expression in the attached part of the model flow (Fig. 2b), where $\eta_{\max} \approx$ constant, coincides with the corresponding expression of Baldwin–Lomax. Test calculations showed good agreement with the experiments if $c = 0.9$. Following as closely as possible the formulation of Baldwin and Lomax,[6] $(\mu_t)_{\text{outer}}$ is defined from

$$(\mu_t)_{\text{outer}} = C_{\text{cp}}(0.0168\rho F_{\text{wake}}\gamma)$$
$$F_{\text{wake}} = \text{the smaller of} \begin{cases} \eta_{\max} F_{\max} \\ \dfrac{0.9\eta_{\text{ref}}^2 F_{\max}}{\eta_{\max}} \end{cases} \tag{7}$$

If these relations are applied to the model flow (Fig. 2a), F_{wake} is equal to the new expression along the attached boundary layer and the separation vortex, until its reattachment. Between reattachment and the fin, F_{wake} is equal to the standard Baldwin–Lomax expression, because $\eta_{\max}$ is very small, almost zero, in this region (the velocity profile is flat). The new relation will be evaluated after presentation of the second model.

Model 2: Inverse Dependence of Eddy Viscosity on $\eta_{\max}$ $F_{\max}$

As mentioned in the Introduction, according to recent work,[10] a low-turbulence tongue exists under the conical separation vortex of a strong swept-shock/turbulent boundary-layer interaction. This tongue creates a mixed-type separation bubble: turbulent in the region of the separation line and almost laminar between the secondary vortex and the reattachment line. This type of separation is not simulated accurately with the algebraic turbulence models usually used. Reliable results give only a version of the Baldwin–Lomax model, in which the vortex is excluded from estimation of the eddy-viscosity coefficients. Actually, in the region of the low-turbulence tongue, this version predicts very small values of the eddy-viscosity coefficient.

As mentioned in the prior section, the wake function of the Baldwin–Lomax model is proportional to the minimum of $F_{w1} = \eta_{\max} F_{\max}$ and $F_{w2} = \eta_{\max}/F_{\max}$ and, in the separation domain, the function F_{w2} is applied, which has roughly an inverse dependence on the maximum vorticity. Still, the level of F_{wake} in the region of the low-turbulence tongue is higher than that required for a realistic simulation of these types of flows.

This leads to the conclusion that to follow the physics of flow, a wake function is required that will take very small values between the secondary vortex and the reattachment region, but in the region of the separation point will have a variation comparable with that of the standard Baldwin–Lomax relations. Fortunately, the function $F_{w1} = \eta_{\max} F_{\max}$ presents a peak close to the core of the vortex (because in this region $F_{\max}$ and $\eta_{\max}$ have large values). This means that the inverse of this function has very small values in the region of the vortex core and higher ones close to the separation and reattachment points. Thus, selection of the inverse of $F_{\max}\eta_{\max}$, properly scaled by F_{ref} and η_{ref}, is a good choice. To avoid very small values of the wake function in the region of the separation point, this new relation is applied a little downstream of this point. The proposed expression is

$$F_{\text{wake}} = \eta_{\max} F_{\max} \quad \text{if} \quad \eta_{\max} < 1.03\eta_{\text{ref}}$$
$$F_{\text{wake}} = \frac{a(\eta_{\text{ref}} F_{\text{ref}})^2}{\eta_{\max} F_{\max}} \quad \text{if} \quad \eta_{\max} > 1.03\eta_{\text{ref}} \tag{8}$$

For definition of the value of the constant a, a parametric numerical application was done, which led to the value $a = 3.0$.

IV. Evaluation of the New Relations

For evaluation of the new relations that were developed in the prior section, the fin–plate experiments performed in the Supersonic Wind Tunnel Facility of the Pennsylvania State University by G. Settles and his associates are used. These tests are well documented in a NASA Report of Settles and Dodson.[11] The measurements include skin friction and wall flow-angle distribution along a circular arc at radius $R = 88.9$ mm from the leading edge of the fin, as well as wall pressure distribution, along a circular arc at radius $R = 101.1$ mm. The skin friction data were produced by the recently developed laser interferometer skin friction technique. The flow angle distribution was extracted from pictures of the pattern of skin-friction lines (obtained by using a kerosene-lampblack visualization technique). The characteristic parameters of the flows that are simulated in this paper are $M_0 = 3.98$, $Re = 6.79 \times 10^7$/m, and fin angle $\alpha = 16$ and 20 deg and $M_0 = 3.03$, $Re = 6.19 \times 10^7$/m, and $\alpha = 16$ deg. The thickness of the boundary layer upstream of the interaction is $\delta_0 = 3$ mm.

Numerical Method, Boundary Conditions

The Reynolds-averaged Navier–Stokes equations, with the x derivative (streamwise direction) of the viscous terms ignored, are solved at the interior grid points of a mesh. A second-order central differencing is applied to the implicitly treated viscous fluxes. The inviscid fluxes are determined by the upwind total variation diminishing scheme of Yee and Harten,[16] which uses Roe's[17] approximate Riemann solver and Harten's second-order modified flux approach. Alternating Gauss–Seidel relaxation in the streamwise direction is employed. Details of the flow solver are given in Ref. 1.

Because of the simplicity of the geometry of the fin–plate configuration, the mesh was generated algebraically. A clustering was applied close to the plate and to the fin for adequate resolution of the viscous effects. In each crossflow direction plane (z, y directions) 105×111 points are used, whereas in the streamwise x direction there are 77 grid planes uniformly spaced, with $\Delta x = 0.5\delta_0$, where δ_0 is the thickness of the boundary layer at the start of calculation. The inflow plane is located at a distance equal to $2\delta_0$ upstream of the leading edge of the fin and the downstream boundary at $x = 36.5\delta_0$. The height of the computational field is $9.23\delta_0$. The width is uniform before the fin, equal to $10.9\delta_0$, but from there on it increases to $z = 29.4\delta_0$ at the outflow plane. The mesh is very fine (897,435 points), especially in the direction normal to the plate. More particularly, 69 points are used for simulation of the undisturbed boundary layer; the minimum value of y^+ at the first point off the plate is 0.15 and its maximum value is equal to 0.5. Initially, 95 points in the y direction and minimum $y^+ = 0.5$ were used. For these values, the level of the skin friction upstream of the interaction was too high. Increasing the number of points to the value 111 and reducing the minimum y^+ to 0.15 resulted in a stable solution that did not change when the minimum y^+ was further decreased to 0.075.

The boundary-layer profile upstream of the interaction region is used as a boundary condition on the inflow plane as well as an initial condition of the flow field. This profile was calculated by a two-dimensional procedure, from the leading edge of the flat plate to the edge of the fin. The profile was similar to the experimental one. Furthermore, the thickness of the undisturbed boundary layer, δ_0, is the length scale of the interaction. The gradients of the flow parameters are set equal to zero on the far field (upper and lateral boundaries) and on the outflow boundary. The walls are assumed impermeable, and no-slip boundary conditions are applied. The pressure gradient normal to the walls is taken equal to zero as well as the temperature gradient (the walls are assumed adiabatic).

With regard to the procedure of calculation of the eddy-viscosity coefficient, the derivation of the two new relations for the eddy-viscosity coefficient is based on the crossflow model shown in Fig. 2. This flow model has a two-dimensional appearance but a three-dimensional structure. Because the crossflow plane is normal to the main flow direction, the Baldwin–Lomax eddy-viscosity parameters ($F_{\max}$, $\eta_{\max}$) remain constant along the undisturbed part of the boundary layer. Thus, any point in this region is suitable to be defined as the reference one. For calculation of the eddy-viscosity coefficient, marching in the streamwise x direction is done. At each streamwise position (denoted by the index I), the eddy-viscosity coefficients are calculated in the crossflow plane (J, K). Index K corresponds to coordinate y (normal to the plate) and J corresponds to z (away from the fin). Before the eddy-viscosity relations are applied, reference J is defined. As the numbering of J starts from the fin, the reference J is chosen close to $J_{\max}$ where the flow is attached, i.e., $J_{\text{ref}} = (J_{\max} - 2)$ to $(J_{\max} - 5)$. It is evident that the parameters F_{ref}, η_{ref} vary along the streamwise direction, because the boundary layer develops in this direction.

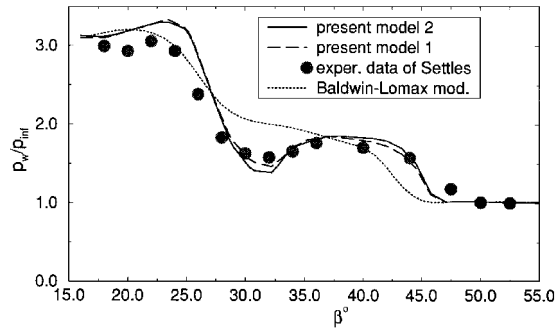

a) $M_0 = 3.0$ and $\alpha = 16$ deg

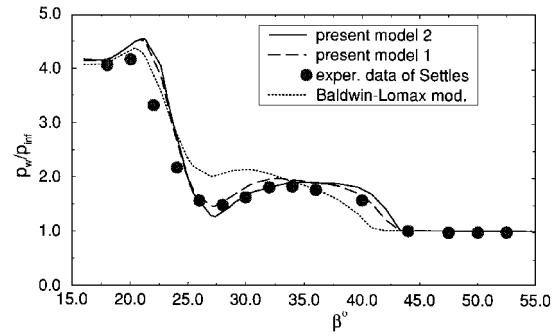

b) $M_0 = 4.0$ and $\alpha = 16$ deg

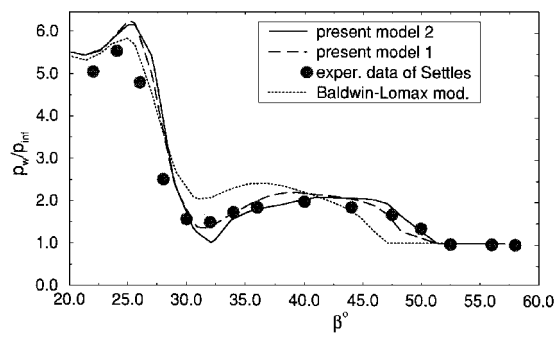

c) $M_0 = 4.0$ and $\alpha = 20$ deg

Fig. 3 Wall pressure predictions.

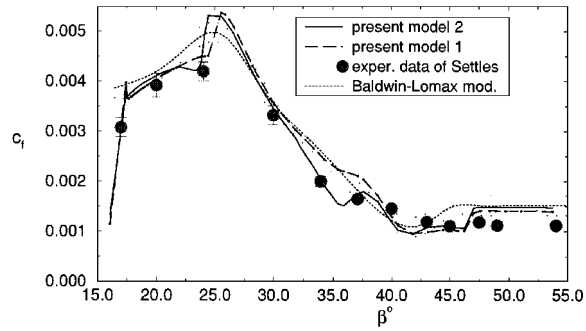

a) $M_0 = 3.0$ and $\alpha = 16$ deg

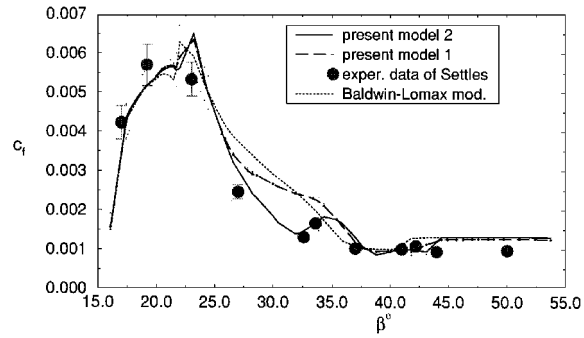

b) $M_0 = 4.0$ and $\alpha = 16$ deg

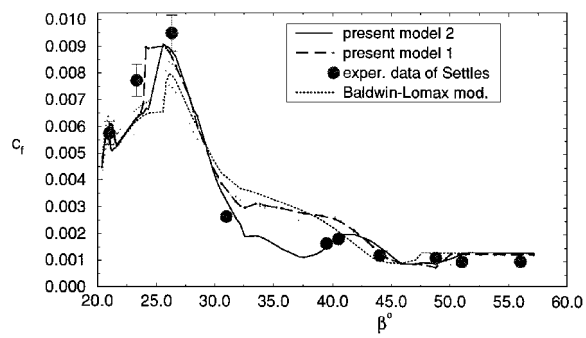

c) $M_0 = 4.0$ and $\alpha = 20$ deg

Fig. 4 Skin-friction predictions.

Comparison with Experiments

As mentioned before, Settles and Dodson,[11] in the database they compiled, give the plate pressure measured along a circular arc of radius $R = 101.6$ mm from the leading edge vs the conical angle β. This angle is measured from the fin leading edge with respect to the freestream direction. In the computational plate, we have found numerically which points of the mesh lie between the arcs R at -0.5 mm, and R at $+0.5$ mm. In these points, the pressure was calculated. The curves these points form are not very smooth, but there is no alternative technique to apply, because very few grid points lie on the circular arc in which the pressure or the other flow parameters were measured. The experimental and the computed wall pressure distributions are compared in Fig. 3 for the three test cases examined, i.e., $M_0 = 3.03$, fin angle $\alpha = 16$ deg and $M_0 = 3.98$, $\alpha = 16$ and 20 deg. The solutions found by application of the Baldwin–Lomax turbulence model are also included. It is shown in Fig. 3 that the results based on the two new eddy-viscosity models agree very well with the experimental evidence. For the extent of the interaction the predictions coincide with the experimental data, with the exception of the reattachment region where the theoretical predictions provide higher values. Also, in the case of the $M_0 = 3.03$ and $\alpha = 16$ deg calculations, both models predict a little shorter interaction length than the experimental one. The agreement between the three solutions based on the Baldwin–Lomax model and the experiments is poor. The spanwise extent is shorter, whereas the local minumum near $\beta = 27-32$ deg (which occurs because of the high reverse velocity of the vortex) is not predicted. There is agreement only in the level of the reattachment pressure. If the two new models are compared in detail, the conclusion is that model 2 tends to predict longer interaction length and smaller local minimum pressure than model 1.

The skin friction comparisons along the measurement arc ($R = 89$ mm) are shown in Fig. 4. Major differences exist between the predictions of the two new models. Only the second model shows good agreement with the experimental evidence. Remarkable in this case is the prediction of the secondary peak (at $\beta = 35-42$ deg) close to which, according to Kim et al.,[7] the secondary vortex lies. This peak is not properly modeled in the solutions based on model 1 and is not present at all in the solutions of the Baldwin–Lomax model. This is an indication that the secondary separation is predicted properly only by model 2. Note that at the reattachment region all our solutions predict a peak. There are not enough experimental points in this region to verify this feature. However, in a picture of the oil-film interference-fringe pattern, which Kim et al.[7] include in their paper, a strong fringe peak is clearly seen near the fin. According to those authors, the fringe pattern may be regarded as being qualitatively indicative of the actual skin-friction distribution. A detailed analysis of the flowfield (not included in the present paper) has shown that the region of disagreement of the two new models is exactly the region occupied by the low-turbulence tongue. Away from this critical region the two models give more or less similar results.

Figure 5 shows the angles of the surface skin-friction lines, ϕ, plotted vs β along the measurement arc ($R = 89$ mm). The local

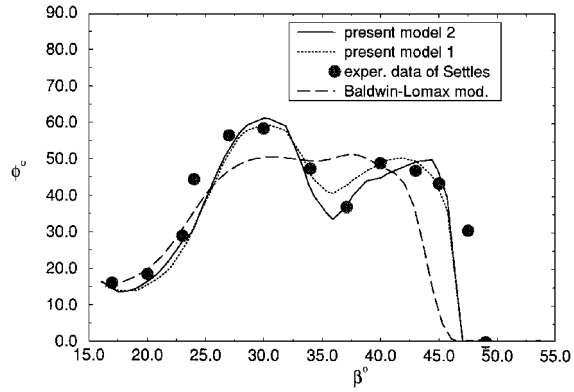

a) $M_0 = 3.0$ and $\alpha = 16$ deg

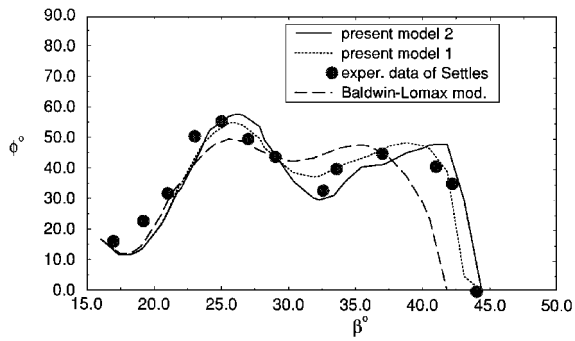

b) $M_0 = 4.0$ and $\alpha = 16$ deg

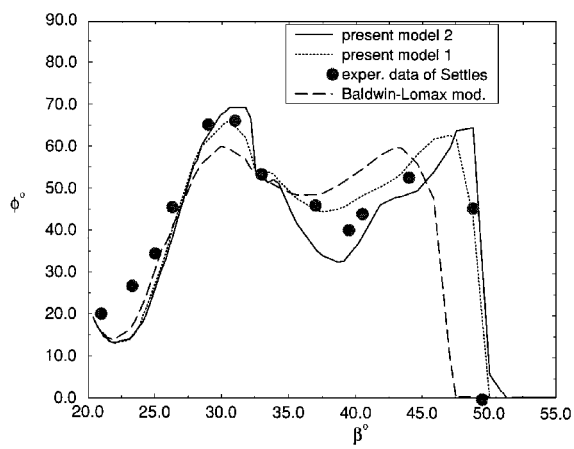

c) $M_0 = 4.0$ and $\alpha = 20$ deg

Fig. 5 Predictions of flow angle at the wall.

minimum at $\beta = 33$–39 deg corresponds to the secondary separation line. The accuracy of the theoretical predictions of model 2 may be considered as good. In the first test case (Fig. 5a), there is a minor disagreement with the experiments in the start of the interaction ($\beta = 47$ deg). Also, in the third test case (Fig. 5c) an overprediction of the minimum value in the region of the secondary separation line is observed. Regarding model 1, away from the region of the secondary vortex, the predicted results are comparable to those of model 2 in all test cases. However, in the region of the secondary vortex there is a systematic underprediction of the flow angle. Finally, the solutions that are based on the Baldwin–Lomax turbulence model underpredict the extent of interaction and the turning of the skin-friction lines in the region of secondary separation.

V. Calculation of a Symmetric Crossing Shock Interaction

A crossing shock-wave/turbulent boundary-layer interaction appears about a configuration consisting of two fins, or wedges, attached normally to a flat plate. The resulting flow is very complicated, even if the fins are symmetric. The computational aspects of the crossing shock interactions are examined by Knight.[2] The flow basically consists of the two counter-rotating quasiconical vortices, which are generated by the individual single fins, and the overlying shock structure. The initial flat conical vortices interact and gradually become vertically oriented in a mushroom-shaped separation region, which occupies a major portion of the exit area of the dual-fin geometry. The two λ-shock structures, which are subjected to mutual interaction and to reflection on the fins, are also very complicated. Evidently, the crossing shock configuration is a severe test for a turbulence model. Because the pair of vortices before their confluence follows the physics on which the development of model 2 is based, the model in this section is applied to a crossing shock test case that other researchers have computed recently.

Settles and Dodson[11] include in their experimental data a strong $M_0 = 3.98$ interaction generated by two symmetric fins placed on a flat plate at 15 deg. The flow conditions are similar to those examined in the prior section for the Mach 4 test case (geometry, boundary layer data). However, various values are cited in other related works for the Reynolds number. We have taken $Re = 7.6 \times 10^7$/m, which is the value used by Garrison et al.[18] A nominal value for the boundary layer thickness, equal to $\delta_0 = 3.5$ mm, is assumed in the database. The width of the channel at the fin leading edge is 9.63 cm, except for skin-friction measurements where it is 10.5 cm. The fins are located 21.3 cm downstream of the plate leading edge. The height of the fins is 8.25 cm.

The calculation procedure described in the prior section for the single-fin cases was also used in the crossing shocks. The only difference is the application of a symmetry condition along the centerline of the plane (normal velocity component equal to zero). Also, the grid described previously was used ($77 \times 111 \times 105$ points) but adapted to the new geometry, which in addition to the fins includes a downstream extension (30 deg) for a smooth outflow condition. This concept was introduced by Garrison et al.[18] In the present case, the streamwise spacing of the grid was $\Delta x = 0.59\delta_0$. Also, normal to the plate direction the minimum y^+ was equal to 0.48.

Settles and Dodson[11] give the measured wall pressure and skin friction along the centerline of the channel as well as the skin friction in a cross section located at $x/\delta_0 = 25.3$. Comparison of our calculated results with these parameters is given in Fig. 6. Starting from the wall pressure, it is shown in Fig. 6a that the calculations based on turbulence model 2 follow the experimental data very closely. These is only a small disagreement in the level of the maximum value, which our calculations underpredict. The agreement of the skin-friction coefficient along the centerline (Fig. 6b) is partial. First, the initial drop toward separation and the subsequent steep recovery are predicted rather well. However, the calculation fails to reproduce the existing plateau, which seems to be indicated by the experiment, after the recovery. It is of course not clear from only three points whether there really exists a plateau in the flow. Considering the good prediction of the pressure in the region of disagreement ($x/\delta_0 = 28.0$–36.0), some details of the flow very close to the wall need more clarification. A similar, but not identical, condition is observed in the calculations of Gaitonde and Shang.[19] The computed skin-friction coefficient along the crossflow cut (Fig. 6c) is closer to the experimental data, although again there are some details that are not simulated correctly. Finally, in Fig. 7, the computed and experimental surface streamline structures are compared. The agreement is good. All the major features of the flow have been reproduced efficiently, better than the predictions presented by Gaitonde and Shang,[19] which were based on the regular Baldwin–Lomax and a κ–ε turbulence model.

A fundamental issue related to turbulence modeling is the existence or not of the low-turbulence tongue below the interacting pair of the vortices. This issue is examined in the DLR internal report (Ref. 20) on which the present paper is based. There it is shown that after merging of the two separation vortices the low-turbulence tongues are formed; farther downstream the lifted combined structure, which gradually takes a mushroom-like shape, sits on air that originally has very low turbulence. It is remarkable that the $y/\delta_0 = 0.80$ stream surface and the lower one ($y/\delta_0 = 0.68$) at the end of the fins run through the central channel of the structure and form an "umbrella."

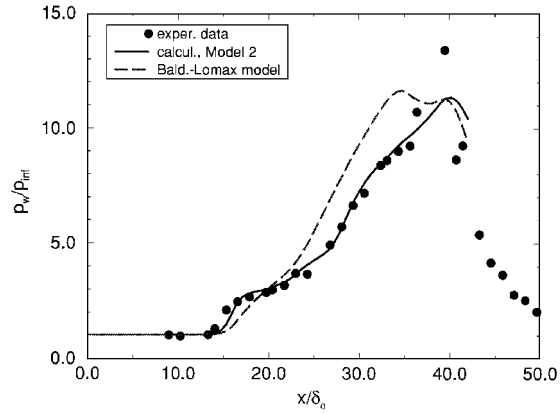

a) Centerline wall pressure

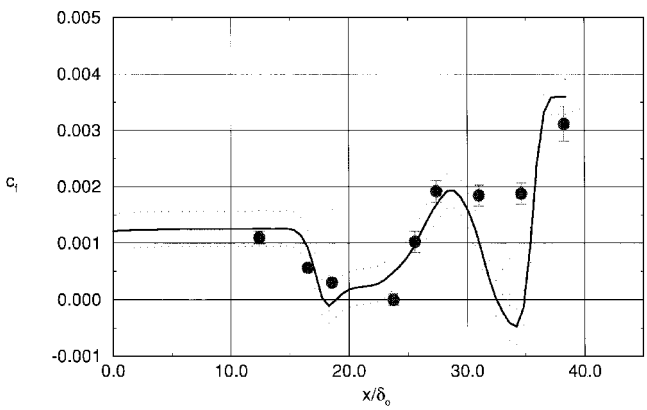

b) Centerline skin friction

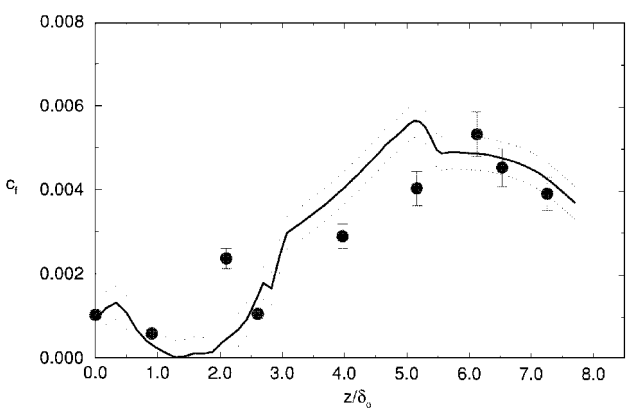

c) Skin friction at cross section $x/\delta_0 = 25.3$

Fig. 6 Comparison of calculations with experiments.

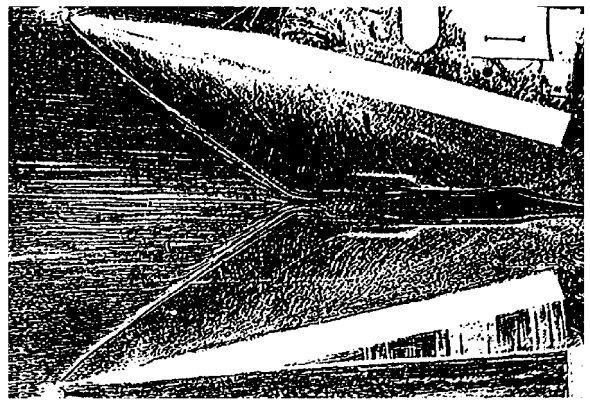

a) Experimental

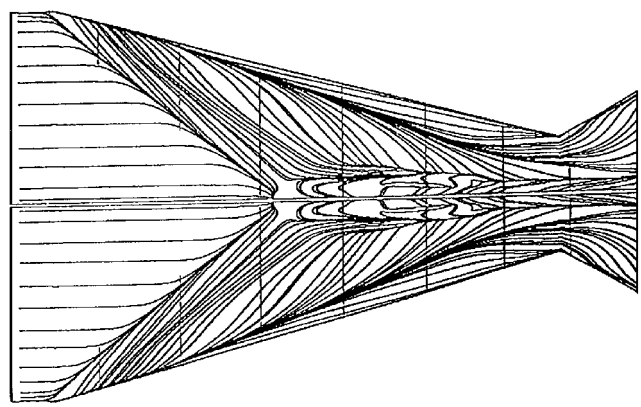

b) Calculated, turbulence model 2

Fig. 7 Surface flow pattern.

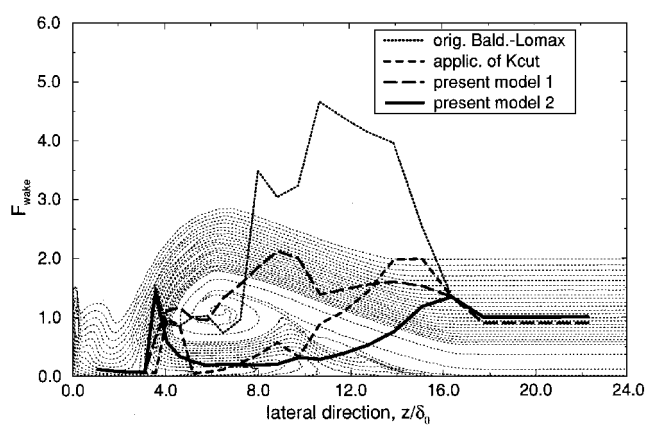

Fig. 8 Comparison of F_{wake} at cross section $x/\delta_0 = 28.1$.

VI. Discussion and Conclusions

The application of two new eddy-viscosity relations in the calculation of some of the single- or double-fin–plate flows, which have been studied experimentally at Pennsylvania State University, resulted in quite accurate results, much closer to the experimental data than those found by application of the Baldwin–Lomax[6] turbulence model. In the first of these new relations, the eddy viscosity across the viscous layer has a linear variation on the maximum vorticity; in the second, there is an inverse dependence on the original wake function of Baldwin–Lomax. As anticipated, the second model is more appropriate than the first one for numerical simulation of the quasiconical flow, which is established about a fin–plate configuration, because it predicts very small eddy-viscosity coefficients in the low-turbulence tongue that exists below the core of the conical separation vortex.

For evaluating the differences between the eddy-viscosity coefficients calculated by the two new relations, it is sufficient to compare the corresponding wake functions. For completeness, the wake functions given by the Baldwin–Lomax model and the cutoff model[10] are included in the comparison. For one of the examined test cases ($M_0 = 3.98$ and $\alpha = 16$ deg), the variation of the function F_{wake} along a crossflow plane ($x = 28.1\delta_1$) is shown in Fig. 8 for the aforementioned turbulence models. In the particular station the conical flow has developed completely, i.e., the secondary vortex has appeared. The values of F_{wake} have been nondimensionalized by its value at the region where the flow is attached. It is shown in Fig. 8 that all the examined turbulence models provide similar values for the function F_{wake} in the regions of the separation and reattachment points. However, the predicted values differ considerably between these regions. The Baldwin–Lomax model predicts the largest values of F_{wake} in the separation region. The values calculated by the linear relation (model 1) are less than half the corresponding values of the Baldwin–Lomax model. Much smaller values are predicted by the inverse relation (model 2) and the cutoff model. These two models provide particularly small values in the region of the low-turbulence tongue below the core of the vortex. Model 2 predicts the smallest eddy-viscosity values in the region of the secondary separation vortex. The observed variation of the wake function in the

region of the low-turbulence tongue is consistent with the level of accuracy of the various turbulence models examined in Fig. 8. Indeed, the most accurate results are given by model 2. This model predicts correctly the extent of interaction and the variation of the various flow parameters in the region of the secondary separation. Quite accurate results have also been obtained for some of the examined flow cases with the cutoff model (see Refs. 8 and 10). However, this model is not so easy to use because of the difficulty to define accurately the cutoff distance during the computation procedure. Model 1 is less accurate than these two models. The flow in the secondary-vortex region is not simulated very correctly by this model. Finally, the Baldwin–Lomax model is the least accurate of all the models examined. It underpredicts the size of the interaction domain and fails to predict the secondary separation.

Note that the reviewed turbulence models, with the exception of the Baldwin–Lomax model, require the definition by the user of a cutoff distance or a reference point. The Baldwin–Lomax model is easier to apply because the eddy-viscosity coefficient does not depend on reference data; however, its accuracy is not comparable with that of the others. Examining in detail the modeling introduced in the present work, the reader is reminded that according to the procedure of calculation of the eddy-viscosity coefficient, outlined in Sec. IV, marching in the streamwise x direction is done and at each streamwise position the eddy-viscosity coefficients are calculated in the corresponding crossflow plane. The parameters F_{ref}, η_{ref} vary along the streamwise direction, because the boundary layer develops in that direction. This computation procedure ensures that the scaling factors of the eddy-viscosity coefficient vary along the streamwise direction of a fin–plate flow, following the development of the undisturbed boundary layer. However, there are flow configurations in which it is not possible to define the required sequence of reference points along the streamwise direction. Such an example is the symmetric crossing shock-wave/turbulent boundary-layer interaction, which was calculated in Sec. V. In this case, the only remaining possibility is application of constant reference parameters in the whole flowfield. For a reference position, a point upstream of the fins close to the inflow plane may be selected. This topic is covered in Ref. 20.

In closing, I will try to answer the obvious question about the applicability of the present turbulence modeling to other types of flows. A distinction should be made between model 1 and model 2. The inverse-variation formula [Eq. (8)] is appropriate only for estimation of the eddy-viscosity coefficient in three-dimensional flows characterized by the appearance of extensive crossflow separation (generation of crossflow vortices). This type of flow is not established only in a swept shock-wave/turbulent boundary-layer interaction, but it is also observed in flows about slender bodies at high incidence. Indeed, crossflow separation occurs when fluid flowing circumferentially from the windward to the leeward side of such a body separates from the sides of the body along a line roughly parallel to its longitudinal axis. The fluid rolls up and forms two primary vortices on the leeward side on both sides of the symmetry plane. Similar vortices appear also in the high-angle-of-attack flow about a delta wing. The strong similarity of the flowfields indicates that Eq. (8) is also appropriate for calculation of the eddy viscosity in the separation region of a flow about a slender body or delta wing. However, this applicability must be assessed, because in these types of flow the boundary layer develops along the circumferential direction and, hence, selection of the appropriate position of the reference points is not obvious. In more complex configurations, like complete aircraft, it is more efficient to use the present model in a multiblock scheme, restricting its application to those regions where strong crossflow separation occurs. Then the difficulty associated with definition of the reference points will be alleviated. Also, convergence is faster if the present model is applied not from the beginning of a computation but later when an approximate solution is available (based on the Baldwin–Lomax model).

With regard to model 1 [Eq. (7)], there is no particular assumption about its form other than the requirement to relate the eddy-viscosity coefficient linearly with a boundary-layer parameter. Again, a particular study is necessary for assessing the applicability of the model in other types of flows. Finally, in the present work I have estimated the thickness of the boundary layer in the region of the shock-wave/boundary-layer interaction, where multiple maxima exist in the moment of vorticity profiles, by applying the following rule: in a crossflow plane, the thickness of the viscous layer above the point of maximum value of the moment of vorticity remains constant along the interaction. This rule is based on practical observations and it is approximate. Still I believe it is useful for application to other types of flows where shock waves and mixing layers exist.

Acknowledgments

This work was done while the author was a visiting scientist at DLR, from the Hellenic Air Force Academy, as recipient of a research fellowship awarded by the European Union within the Human Capital and Mobility programme. The assistance of the European Union is acknowledged as well as that of the DLR, which provided the computational means and all the required support. The author wishes to thank W. Kordulla for his invitation to work in the Numerical Department of the Institute of Fluid Mechanics and for his constructive comments. Thanks are also due to D. Schwamborn, head of the Numerical Department, for his detailed suggestions and comments regarding this paper.

References

[1]Panaras, A. G., "Numerical Investigation of the High-Speed Conical Flow Past a Sharp Fin," *Journal of Fluid Mechanics*, Vol. 236, 1992, pp. 607–633.

[2]Knight, D. D., "Numerical Simulation of 3-D Shock Wave Turbulent Boundary Layer Interaction," AGARD-R-792 Paper 3, Aug. 1993.

[3]Settles, G. S., "Swept Shock/Boundary-Layer Interactions—Scaling Laws, Flowfield Structure, and Experimental Methods," AGARD-R-792 Paper 1, Aug. 1993.

[4]Panaras, A. G., "Review of the Physics of Swept-Shock/Boundary-Layer Interactions," *Progress in Aerospace Science*, Vol. 32, 1996, pp. 173–244.

[5]Cebeci, T., and Smith, A., *Analysis of Turbulent Boundary Layers*, Academic, New York, 1974.

[6]Baldwin, B. S., and Lomax, H., "Thin Layer Approximation and Algebraic Model for Separated Turbulent Flows," AIAA Paper 78-257, Jan. 1978.

[7]Kim, K. S., Lee, Y., Alvi, F. S., Settles, G. S., and Horstman, C. C., "Laser Skin Friction Measurements and CFD Comparison of Weak-to-Strong Swept Shock/Boundary Layer Interaction," *AIAA Journal*, Vol. 29, No. 10, 1991, pp. 1643–1650.

[8]Panaras, A. G., and Stanewsky, E., "Numerical Study of Secondary Separation in Glancing Shock/Turbulent Boundary Layer Interactions," AIAA Paper 92-3666, July 1992.

[9]Degani, D., and Schiff, L. B., "Computation of Turbulent Supersonic Flows Around Pointed Bodies Having Crossflow Separation," *Journal of Computational Physics*, Vol. 66, 1986, pp. 173–196.

[10]Panaras, A. G., "The Effect of the Structure of Swept Shock-Wave/Turbulent Boundary-Layer Interactions on Turbulence Modelling," *Journal of Fluid Mechanics* (to be published).

[11]Settles, G. S., and Dodson, L. J., "Hypersonic Shock/Boundary-Layer Interaction Database," NASA CR-117577, April 1991.

[12]Hung, C. M., and MacCormack, R. W., "Numerical Solution of Three-Dimensional Shock Wave and Turbulent Boundary-Layer Interaction," *AIAA Journal*, Vol. 16, No. 10, 1978, pp. 1090–1096.

[13]Stock, H. W., and Haase, W., "Determination of Length Scales in Algebraic Turbulence Models for Navier–Stokes Methods," *AIAA Journal*, Vol. 27, No. 1, 1989, pp. 5–14.

[14]Johnson, D. A., "Nonequilibrium Algebraic Turbulence Modelling Considerations for Transonic Airfoils and Wings," AIAA Paper 92-0026, Jan. 1992.

[15]Alvi, F. S., and Settles, G. S., "A Physical Model of the Swept Shock/Boundary-Layer Interaction Flowfield," *AIAA Journal*, Vol. 30, No. 9, 1992, pp. 2252–2258.

[16]Yee, H. C., and Harten, A., "Implicit TVD Schemes for Hyperbolic Conservation Laws in Curvilinear Coordinates," *AIAA Journal*, Vol. 25, No. 2, 1987, pp. 266–274.

[17]Roe, P. L., "Approximate Riemann Solvers, Parameters, Vectors and Difference Schemes," *Journal of Computational Physics*, Vol. 43, 1981, pp. 357–372.

[18]Garrison, T. J., Settles, G. S., Narayanswami, N., and Knight, D. D., "Structure of Crossing-Shock-Wave/Turbulent-Boundary-Layer Interactions," *AIAA Journal*, Vol. 31, No. 12, 1993, pp. 2204–2221.

[19]Gaitonde, D., and Shang, J. S., "Structure of a Turbulent Double-Fin Interaction at Mach 4," *AIAA Journal*, Vol. 33, No. 12, 1995, pp 2250–2258.

[20]Panaras, A. G., "Algebraic Turbulence Modelling for Swept Shock-Wave/Turbulent Boundary-Layer Interactions," DLR-IB-223-96 A 22, March 1992.

J. Kallinderis
Associate Editor